Microscopic Signature of a Microgel Volume Phase Transition

B. Sierra-Martín,[†] Y. Choi,[‡] M. S. Romero-Cano,[†] T. Cosgrove,[‡] B. Vincent,[‡] and A. Fernández-Barbero*,[†]

Department of Applied Physics, University of Almería, 04120-Almería, Spain, and School of Chemistry, University of Bristol, Cantock's Close, Bristol BS8 1TS, U.K.

Received May 19, 2005; Revised Manuscript Received September 1, 2005

ABSTRACT: This paper discusses the dynamics of water molecules in poly(NIPAM) microgel dispersions. ^{1}H NMR spectroscopy is used to determine the self-diffusion coefficient of the water molecules. The capability of the microgel particles to restrict the motion of water molecules depends on the degree of swelling, as determined by dynamic light scattering. The dependence of molecular diffusion on the network density is established. This is tested against Yasuda's free volume model and Ogston's obstruction model, which have been modified to account for the dependence of the network pore size on the extent of swelling.

1. Introduction

It is known that confinement can induce unusual behavior in the properties of matter.[1−3] Scientific interest and important technological applications have produced an extensive research field on this topic, bringing together disciplines as diverse as nanotechnology,[4] protein handling[5] and nanocomposites.[6] Macroscopic hydrogels and microgels have been widely used for the uptake, encapsulation and release of biological macromolecules and technologically "active" molecules.[7−10] However, as far as we know, there have been very few[11,12] previous studies of how the motion of water molecules is restricted in this kind of systems.

Thermosensitive poly(*N*-isopropylacrylamide) [poly(NIPAM)] is one of the most frequently studied microgels. These systems exhibit a reversible, continuous volume phase transition at a lower critical solution temperature (LCST) around 32 °C.[13] The transition is associated with the decreasing solvency of water for poly(NIPAM) with increasing temperature. The degree of swelling is controlled by the free energy changes associated with (i) mixing of the polymer and water molecules and (ii) the network elasticity, as described, for example, by the Flory−Huggins theory.[14] As microgel particles collapse, so water molecules are expelled out of the polymer network and conformational changes take place. It is accepted that water molecules in hydrogels exists in different states, known as "bound", "intermediate", and "free" water.[15] Evidence for the existence of bound water is the presence of nonfreezable water within hydrogels.

The aim of this paper is to monitor the dynamics of water molecules confined in poly(NIPAM) microgel particles. Different systems with increasing proportions of cross-linker have been synthesized to vary the confinement conditions. ^{1}H NMR spectroscopy has been used to determine the self-diffusion coefficients of water molecules. Dynamic light scattering (DLS) has been used to determine the degree of polymer network swelling. The relationship between molecular diffusion and network density has been established. This is tested against Yasuda's free volume model and Ogston's obstruction model, which have been modified to account for the dependence of the network pore size on the extent of swelling.

The outline of this paper is as follows. Section 2 describes the experimental systems. Section 3 discusses the two principle experimental methods employed in this paper: dynamic light scattering and NMR ^{1}H spin−spin relaxation time, together with the procedure used to derive self-diffusion coefficients from spin relaxation data. Section 4 contains the experimental results and discussion. Section 5 summarizes the main conclusions.

2. Preparation of PNIPAM Microgels

Poly(*N*-isopropylacrylamide) microgel dispersions were prepared by surfactant-free emulsion polymerization, following the original recipe by Pelton et al.[16] as developed by Crowther et al.[17] N,N′-Methylenebis(acrylamide) (BA) and potassium persulfate (Sigma-Aldrich) were used as the cross-linking monomer and the initiator, respectively. NIPAM (12-x) grams and BA (x) grams were placed in a three-necked, round-bottomed flask equipped with a stirred paddle and a water-cooled condenser. The reaction vessel was filled to 800 mL using deionized ultrapure water (Millipore). The solution was stirred at 70 °C for 20 min at 350 rpm, under a nitrogen atmosphere. Potassium persulfate (0.54 g), dissolved in water, was then added in order to initiate the polymerization reaction. The reaction was maintained for 16 h before cooling (but with continued stirring). The dispersion was then filtered through glass wool and extensively dialyzed against deionized water, using 14000 Da dialysis tubing (Medicell International), until the conductivity of the dialysate was reduced to 1 μS/cm. Poly(NIPAM) dispersions with cross-linker concentrations in the range 0.5−10 wt % BA were prepared using this method. TEM pictures showed the dry particles to be spherical and highly monodisperse (inset of Figure 1).

3. Experimental Methods

Dynamic Light Scattering. The volume phase transition of the particles was monitored as particle size changes using dynamic light scattering (DLS). A Malvern 4700 system, equipped with a 5 mW helium−neon laser (λ = 632.8 nm) was employed, with the scattering angle set at 40°. The temperature was controlled to a precision of ±0.1 °C, using, simultaneously, two thermostats: (i) a Peltier thermocouple located inside the water bath surrounding the sample cell and (ii) circulation of temperature-controlled water through an external aluminum bath chamber. The dispersions were diluted sufficiently to diminish any colloidal interactions (and hence any structure factor contributions), as well as any multiple

* Corresponding author: e-mail: afernand@ual.es.
[†] University of Almería.
[‡] University of Bristol.

10.1021/ma0510284 CCC: $30.25
Published on Web 11/19/2005

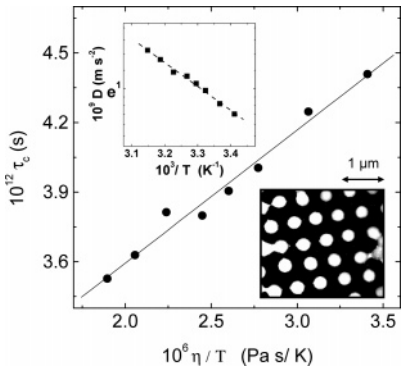

Figure 1. Correlation time as a function of η/T. The correction parameter κ is obtained by fitting the Debye equation, $\tau_c = \tau_0 + (4\pi\kappa a^3/3k)(\eta/T)$, including a free rotation time τ_0. The microviscosity correction parameter κ is calculated from the slope. The top-left inset shows the diffusion coefficient for free water. The slope gives an estimation of the activation energy. In the bottom-right inset a TEM picture for a collapsed microgel (0.5% BA) is shown.

scattering. The mean diffusion coefficient was derived from the intensity autocorrelation function using cumulant analysis and converted into mean particle size via the Stokes−Einstein equation for spherical particles. The mean hydrodynamic diameter was averaged over five single measurements.

NMR ^{1}H Spin−Spin Relaxation Time. Proton NMR relaxation time experiments were performed using a MSL300 Bruker spectrometer. A temperature unit (Bruker VT) controlled the temperature in the magnet bore using a cryostat gas flow and a thermocouple placed just below the sample cell. The temperature was maintained within ± 1 K, following a standard calibration. The polymer concentration was carefully maintained at 4 (w/w) % for all experiments, and provided sufficient sensitivity. The relaxation data were obtained using the standard Carr-Purcell-Meiboom-Gill (CPMG) spin echo sequence.[18,19] The ^{1}H spin−spin relaxation time T_2 was derived using the equation $M_y(n\tau) = M_y(0)\exp(-n\tau/T_2) + B$, where $M_y(n\tau)$ is the instantaneous transverse magnetization between even-pairs of 180° pulses, separated by a time interval τ (τ = 200 μs). $M_y(0)$ is the magnetization immediately following the 90° pulse, n is the number of 180° pairs, and B is the baseline offset. The spacing between pulses is short enough to ensure that diffusion effects are practically eliminated.[20] The NMR experiments were performed over a typical time scale of seconds, which captures the spin relaxation for free and bond solvent molecules. On the other hand, contributions from protons belonging to the polymer network do not contribute, since the typical relaxation time scale of such processes is on the order of milliseconds. Protons signal showed a slight chemical shift, which was always taken into account before the pulse sequence construction.

The NMR transverse relaxation of solvent molecules in a colloidal dispersion may be interpreted assuming rapid exchange between molecules in different environmental states: (i) bound solvent molecules, characterized by a short relaxation time, T_{2b}, and (ii) free solvent molecules in the bulk with a longer relaxation time, T_{2f}.[21] Despite the presence of different relaxation times, corresponding to different molecule states, a single exponential-averaged magnetization curve is observed. The transverse relaxation time is given, in the fast exchange limit, by[22] $1/T_2 = (1 - P_b)/T_{2f} + P_b/T_{2b}$, where P_b is the fraction of bound protons or, more precisely, the fraction of time protons spend in the bound environment, under rapid exchange conditions.

The relaxation process of protons is mainly controlled by dipolar interaction and spin rotation. The spin-rotation contribution to the overall relaxation is estimated to be about 3% (0.003 s^{-1}) at 90 °C.[23] This contribution decreases at lower temperatures and may then be neglected. The spin−spin relaxation rate is written as the summation of two contributions coming from intramolecular and intermolecular dipole−dipole interactions, respectively:

$$\frac{1}{T_2} = \left(\frac{1}{T_2}\right)_{\text{intra}} + \left(\frac{1}{T_2}\right)_{\text{inter}} \quad (1)$$

For isotropic rotational motion the intramolecular dipolar contribution is given by[24]

$$\left(\frac{1}{T_2}\right)_{\text{intra}} = \frac{1}{5}\left(\frac{\mu_0}{4\pi}\right)^2 \gamma^4 \hbar^2 \frac{I(I+1)}{r^6}\left(3\tau_c + \frac{5\tau_c}{1+\omega^2\tau_c^2} + \frac{2\tau_c}{1+4\omega^2\tau_c^2}\right) \quad (2)$$

where μ_0 is the magnetic permeability of vacuum; $\gamma = 2.675 \times 10^8$ rad T^{-1} s^{-1} is the gyromagnetic ratio for protons; r accounts for the distance between protons; $I = 1/2$ is the nuclear spin for protons; $\omega/2\pi$ is the spectrometer frequency; τ_c corresponds to the rotational correlation time and represents the time molecules take to rotate. For low viscosity liquids, composed of small molecules, τ_c is sufficiently short to guarantee $\omega^2\tau_c^2 \ll 1$ (extreme narrowing conditions) and, consequently, the transverse relaxation time does not depend on the magnetic field.

The correlation time is related to the macroscopic viscosity (η) through the corrected Debye equation:

$$\tau_c = \frac{4\pi a^3 \kappa \eta}{3kT} \quad (3)$$

where a is the hydrodynamic radius of the molecules. The parameter κ is a microviscosity correction to the Debye equation for molecular liquids.[25]

Under extreme narrowing conditions, with a uniform distribution of molecules surrounding a given molecule and κ not far from 1, the intermolecular contribution $(1/T_2)_{\text{inter}} \approx (1/T_1)_{\text{inter}}$ is calculated using the Hubbard equation:[26]

$$\left(\frac{1}{T_2}\right)_{\text{inter}} = \frac{3\pi^2\mu_0\gamma^4\hbar^2 N\eta}{40kT}\left[1 + 0.233\left(\frac{b}{a}\right)^2 + 0.15\left(\frac{b}{a}\right)^4 + ...\right] \quad (4)$$

where N is the number of spins per unit volume; a is the hydrodynamic radius of the molecules; b is the distance of protons to the center of the molecule. The intermolecular term contains contributions from the following: (i) the translational motion of molecules (first term in the square brackets) and (ii) the rotation of neighboring molecules (second and third terms). For $b/a \approx 0.5$, the second and third terms represent about 6.8% of the total contribution.

Self-Diffusion Coefficients from Spin Relaxation Data. NMR spectroscopy is used to measure the self-diffusion coefficients of molecules from spin time-relaxation.[27] The rotational correlation time τ_c, determined from time relaxation data, is related to the viscosity and the diffusion coefficient by means of the Debye and Stokes−Einstein equations.

In this section, the method employed to calculate the self-diffusion coefficient is described. It is then applied to free water molecules, as a test, before using it to determine the diffusion coefficients of water molecules confined within the microgel network. Relaxation of water protons is caused by two different mechanisms associated with intramolecular and intermolecular dipolar interactions. The *intermolecular contribution* (eq 4), is calculated using the values for a and b for water[28] (a = 1.38 Å, b = 0.92 Å) and the viscosity of water. The *intramolecular contribution* is obtained using eq 1 from the experimental T_2 values and the calculated intermolecular contribution. Finally, eq 2 is employed to calculate the rotational correlation time, τ_c. The value r = 1.52 Å for protons was used in this equation. The contributions to T_2 and the correlation times, at different temperatures, for free water are summarized in Table 1. Figure 1 is a plot of the correlation time as a function of η/T. The correction parameter κ is obtained

Table 1. Contributions to Total Relaxation Time and Correlation Times of Free Water[a]

T/K	$(1/T_2)$/s^{-1}	$(1/T_2)_{inter}$/s^{-1}	$(1/T_2)_{intra}$/s^{-1}	τ_c/ps
293	0.432	0.126	0.305	4.408
297	0.408	0.114	0.294	4.246
301	0.380	0.103	0.277	4.004
303	0.367	0.096	0.270	3.904
306	0.354	0.091	0.263	3.799
310	0.347	0.083	0.264	3.813
314	0.328	0.076	0.251	3.628
318	0.315	0.070	0.244	3.527

[a] Errors are about 2%.

by fitting to the Debye equation, eq 3. The rotational correlation time is, as expected, a linear function, $\tau_c = \tau_0 + S\eta/T$.

In the ideal limit of very high temperatures, molecular rotation is decorrelated and τ_0 should be zero. However, for finite temperature and small viscosities, a small nonzero τ_0 should result. τ_0 is interpreted as a free rotation time[29] and has to be included in the Debye equation. The microviscosity correction parameter κ is calculated from the slope of the linear fit, $S = 4\pi\kappa a^3/3k$. This leads to $\tau_0 = 2.44$ ps and $S = 5.7 \times 10^{-7}$ K Pa^{-1} and $\kappa = 0.72 \pm 0.05$. The translational diffusion coefficient is expressed by the Stokes−Einstein equation, $D = kT/6\pi a\kappa\eta$, once the microviscosity correction factor, κ, is taken into account. It allows diffusion coefficients for free or confined water molecules to be determined (once the viscosity is calculated from T_2) because of κ depends only on the size and shape of the water molecule. To this end, eqs 1, 2, 4 and the function, $\tau_c = 2.44 \times 10^{12} + 5.7 \times 10^{-7}\,\eta/T$, are combined to give

$$\left(\frac{1}{T_2}\right) = A\left(1.88 \times 10^{-12} + 6.2 \times 10^{-7}\frac{\eta}{T}\right) + B\frac{\eta}{T} \qquad (5)$$

from which the viscosity is calculated. A and B are temperature and viscosity-independent constants, given by

$$A = 2\left(\frac{\mu_0}{4\pi}\right)^2 \gamma^4 \hbar^2 \frac{I(I+1)}{r^6} \qquad (6)$$

$$B = \frac{3\pi^2\mu_0\gamma^4\hbar^2 N}{40k}\left[1 + 0.233\left(\frac{b}{a}\right)^2 + 0.15\left(\frac{b}{a}\right)^4\right] \qquad (7)$$

It is interesting to note that eq 5 is valid since $\tau_c = f(\eta/T)$ depends only on the molecule size and shape. Thus, although it has been derived from data for free water, it is also valid when water molecules are trapped inside the microgel particles. The presence of microgel particles changes η, but not the functional relationship between τ_c and η.

To test this method, the self-diffusion coefficient of free water was first measured and then compared with literature values. At 20 °C a value, $D = (2.2 \pm 0.2) \times 10^{-9}$m^2 s^{-1} was obtained. This agrees reasonably well with the value $D = 2.03 \times 10^{-9}$m^2 s^{-1} reported by Mills[30] (using pulsed field gradient PGSE-NMR).

For pure liquids, the diffusion coefficient is written as $D = c\exp(-E_a/RT)$, where E_a is an activation energy, R, the ideal gas constant and c is a fitting constant. The inset of Figure 1 shows the Arrhenius plot for the diffusion coefficient, leading to $E_a = 18.4 \pm 0.7$ kJ/mol. Mills reported $E_a = 19.6$ kJ/mol (1−15°) and $E_a = 17.6$ kJ/mol (15−45°) for these two temperature ranges. The values obtained in the current work are in good agreement, therefore. It may be concluded, therefore, that diffusion coefficient values may be adequately determined from relaxation times using the described method.

4. Results and Discussion

Molecular Confinement within the Microgel Network. The general purpose of this current study was to study the effect of the confinement conditions on the solvent molecular motion. Several microgels, with different cross-linking densities, were synthesized in order to modify the network pore size, and, hence, also the diffusion of water molecules through the polymer network. Variation in the cross-link density, also leads to changes in the elastic component of the polymer network, changing, not only the maximum extent of swelling of the network, but also the frictional resistance for water molecules to enter or leave the network.

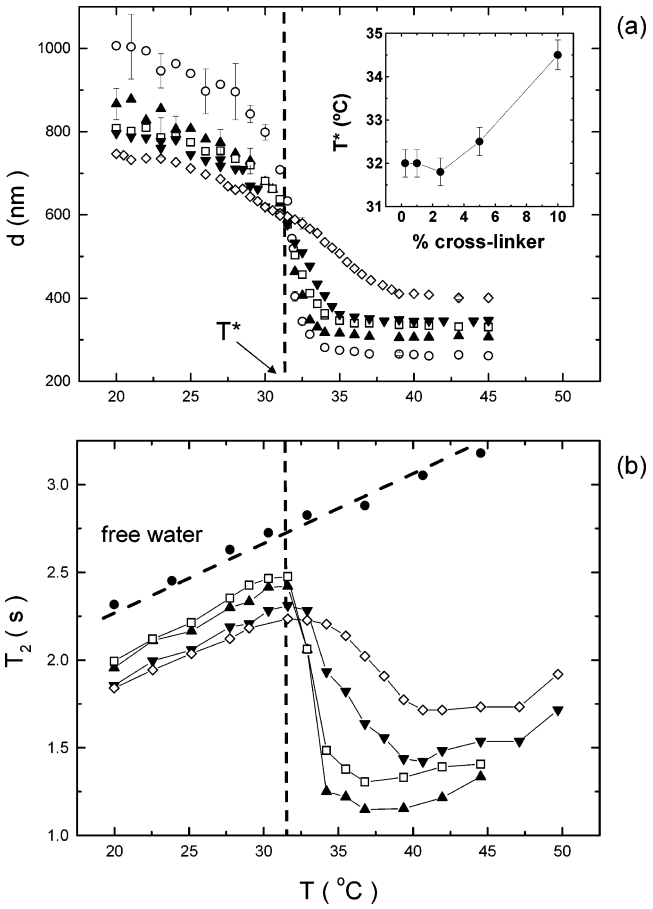

Figure 2. (a) Hydrodynamic diameter for microgels with different cross-linker (BA) content: (○) 0.5%, (▲) 1%, (□) 2.5%, (▼) 5%, and (◇) 10%. T^* is the transition temperature, defined as the maximum of the first derivative. The inset plots the transition temperature against the cross-linking concentration. (b) Temperature dependence of T_2 for free water and PNIPAM microgel dispersions with different cross-linker content: (▲) 1%, (□) 2.5%, (▼) 5%, and (◇) 10%.

To follow the microgel network transition with increasing temperature, the mean particle size was measured using DLS. Figure 2a shows the mean particle size−temperature data for PNIPAM particles of different cross-link density. Figure 2b plots the temperature dependence of T_2 for free water as a reference, and the corresponding to PNIPAM microgel dispersions with different cross-linker content, obtained from NMR measurements, as described above. The swelling process is thermoreversible without any significant hysteresis, and shows that the particle size decreases continuously and monotonically with increasing temperature, eventually reaching a collapsed (temperature-independent) state. The swelling/deswelling plot becomes "sharper" as the cross-linker content diminishes. The phase transition temperature, T^*, defined as that temperature where the first derivative of the plot is a maximum, is located about 32 °C. The transition temperature is independent of the cross-linker concentration for values lower than

about 4%, but increases slightly for higher concentrations, as is represented in the plot at the upper right-hand corner of Figure 2a. For 10% cross-linking, the presence of the cross-linker increases T^* by about 2.5 °C. This increase indicates that the interaction between the polymer chains and the solvent molecules changes when the amount of cross-linking molecules is high enough, and it is related to the increasing solubility of the BA moieties at higher temperatures, as suggested in previous work[31−33].

T_2 for free water increases with increasing temperature due to the direct influence of temperature on molecule diffusivity (Figure 2b). For the PNIPAM dispersions, T_2 also increases initially with increasing temperature, following the same trend observed for free water up to about the transition temperature, T^*. Above this value, there is a transition in T_2 to lower values, over the temperature range where the volume phase transition occurs. Finally, above this temperature range, T_2 again shows a slight increase with increasing temperature. The transition for several heating/cooling cycles was reversible, without any hysteresis.

For hydrogels, it is well-known that a fraction of the water is bound to specific sites within the polymer network, while the rest behaves as free water. Lele et al.[15] used an extended lattice-fluid hydrogen-bond theory (LFHB) to predict the bound water content in PNIPAM gels as a function of temperature. In this model, they describe "bound" water molecules, both in terms of hydrogen-bonding associations and also through hydrophobic associations. A sharp change was found in the fraction of bound water molecules. This result was confirmed experimentally by Dong and Hoffman.[34] As a consequence of this effect and considerering eq 1, the measured relaxation time should increase through the volume transition region when the network collapses. However, in Figure 2b the opposite behavior is observed. This implies that, despite the fraction of bound water decreasing, these bound water molecules contribute so strongly to the total relaxation time that the final balance is a reduction of the relaxation time when particles collapse. According to this picture, T_2 changes at the transition band as a direct consequence of changes in molecule confinement; such changes are a signature of the volume phase transition *at the molecular level.*

Below the transition temperature, T_2 has similar values to that for free water. This is due to the low degree of confinement for highly swollen particles. Molecular motion of the water molecules is much more restricted above the transition temperature due to their mechanical arrest caused by the strong polymer−polymer attractive interaction, leading to network shrinkage, and the corresponding smaller pore size. This result agrees with the LFHB theory, which predicts that in the collapsed state about 80% of the water molecules are bound to polymer segments in the network, while in the swollen state the corresponding value is only about 30%.

The microgel size in the swollen state is smaller for microgel particles with a higher cross-linker content. This is a consequence of the greater network elastic component trying to collapse the particles further (Figure 3a). However, there is very little influence of cross-linker content on T_2 (Figure 3b). This result is not surprising since the confinement is not very strong for swollen networks, and any modification of the mesh pore

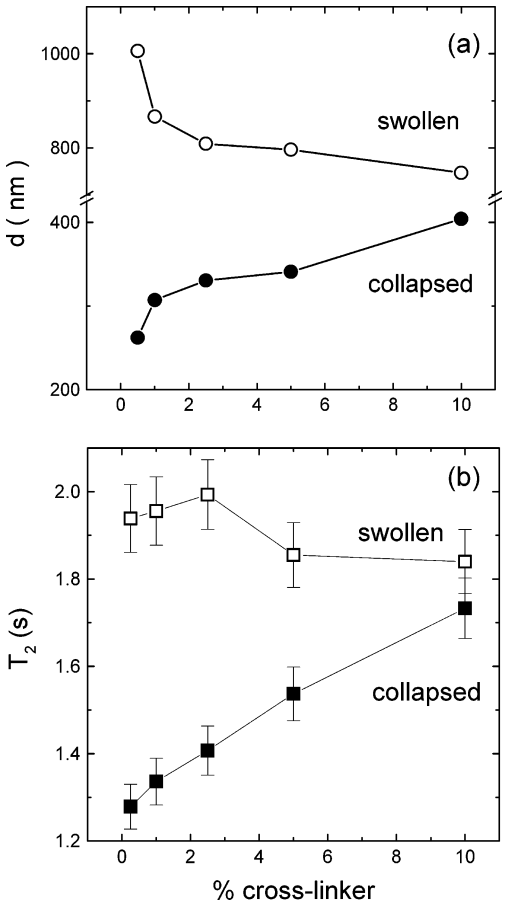

Figure 3. (a) Cross-linker content effect on the final particle size in the swollen and collapsed states. (b) Influence of the cross-linker content on T_2.

size will have only a small effect on the mobility of the molecules, which behave similarly to free molecules. Above the transition temperature, the results are very different. Because of their decreasing solubility, the NIPAM segments try to collapse the particles while the BA segments try to cause extra expansion, which competes to some extent against the effect of the NIPAM. This result agrees with data reported by Hellweg[32] for microgel synthesized in the absence of surfactant. However, it contrasts with the results obtained by Varga et al.[31] who found the collapsed size to be practically independent of cross-linker density. This discrepancy may be due, in part, to the different preparation conditions, since the latter authors synthesized the microgels in the presence of surfactant. The variation in network size with variation in cross-linking has an important influence on the solvent confinement. Figure 3b shows how T_2, for the microgels in the collapsed state, increases as the extent of cross-linking increases. The solvent confinement is controlled by the mesh density.

Mechanical Nature of the Molecular Confinement. The self-diffusion coefficient of the water molecules in a PNIPAM microgel dispersion has been determined using the method developed in section 3. The diffusion coefficients for systems with differing degrees of cross-linking are plotted in the inset of Figure 4. These plots show a behavior similar to those for T_2, that is, increasing monotonically below the transition temperature, decreasing beyond the transition temperature, and then increasing again. To separate the effect of the network volume phase transition from the direct

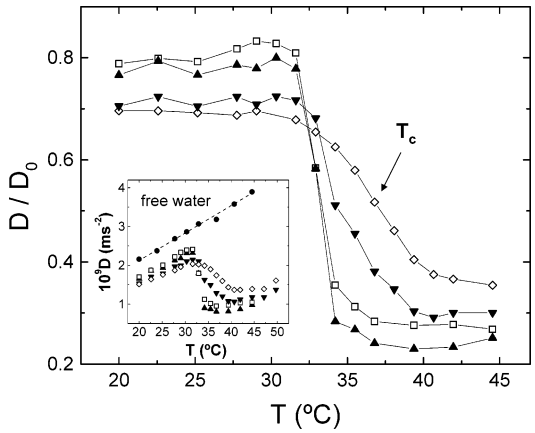

Figure 4. Normalized diffusion coefficient as a function of temperature for microgel particles with different cross-linker content: (▲) 1%, (□) 2.5%, (▼) 5%, and (◇) 10%. The inset plots the diffusion coefficients calculated directly using eq 5 and the Stokes−Einstein equation.

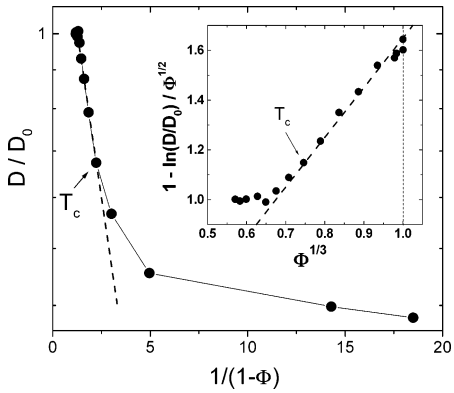

Figure 5. Diffusion coefficient as a function of polymer volume fraction. In the main plot, the data are fitted to Yasuda's free volume model for low Φ. The plot in the inset shows the agreement between the experimental data and the linear behavior predicted by the modified Ogston's obstruction model. T_c defines the temperature at which the diffusion mechanism changes from free volume controlled to network obstruction controlled.

influence of the temperature on D, the self-diffusion coefficients were divided by the free water diffusion coefficient, D_0. Figure 4 shows the normalized diffusion coefficients plotted as a function of temperature. The observed reduction of the molecule translational motion is a microscopic manifestation of the phase transition. As was concluded from the earlier discussion in terms of T_2, bound water strongly influences the value of D.

For lower temperatures, D is virtually constant, even though the polymer network deswells as the transition temperature is approached. Only in the actual region of the transition temperature do water molecules feel any significant confinement, with their mobility decreasing strongly as the mesh size decreases. The diffusion of the water molecules is restricted by the increasing polymer−polymer attractions causing collapse of the microgel network. This effect imposes a restriction on the mobility of the molecules, since this interaction dominates strongly over the polymer−water ones. At temperatures below the transition, D decreases with increasing cross-linker content. However, for higher temperatures, D increases with increasing cross-linker content. This fact indicates that the molecular diffusion is controlled only by the network size, and is independent of the mechanism controlling the network swelling (elasticity below the transition temperature or hydrophobicity above it).

At this point, it is interesting to compare directly the mobility of the water molecules and the network swelling. The diffusion coefficient measured by NMR is plotted against the polymer volume fraction obtained by light scattering. For this purpose, data corresponding to the strongest confinement condition (10% cross-linking) have been used. Figure 5 indicates how the diffusion is most probably controlled by a free volume mechanism at low network compaction, while at higher network densities mesh obstructions control the diffusion. These two mechanisms are indicated in Figure 5. On the main plot, the data have been fitted to Yasuda's free volume model,[35] $\ln(D/D_0) \sim 1/(1 - \Phi)$, for polymer volume fractions below the transition temperature, T_c. This model fails, however, at higher polymer concentrations. The presence of polymer chains reduces molecular diffusion by occupying some of the available free volume. Hence, for swollen microgels ($T < T_c$) the main reduction in water diffusion arises from the polymer chain presence. The data plotted in the inset shows good agreement with the modified Ogston's obstruction model,[36] for higher polymer concentrations. The original Ogston's model predicts the following relation between the diffusion coefficient and he polymer network volume fraction, $D/D_0 \sim \exp([-(r_s + r_f)/r_f]\Phi^{1/2})$, where r_s is the hydrodynamic radius of the solvent molecules; r_f accounts for the radius of the fiber (network). For microgel dispersions, r_f changes with temperature and so, also, with the polymer concentration. The network pore size has been considered to be proportional to the particle size $r_f \sim d$. This hypothesis was previously tested using small-angle neutron scattering.[37] This information is introduced into the model, leading to $-\ln(D/D_0)/\Phi^{1/2} = 1 + B\Phi^{1/3}$, where $B = f(r_s, d_0)$ is a constant when the polymer volume fraction varies as a consequence of temperature changes. The predicted linear behavior is observed for volume fractions corresponding to temperatures higher than T_c. Thus, molecular diffusion is now controlled by obstruction effects caused by the polymer chains. T_c, defined as the temperature at which $|dD/dT|$ reaches its maximum value (see Figure 4), establishes the boundary between the two diffusion mechanisms.

5. Conclusions

The confinement of solvent molecules in a microgel in the region of the volume transition has been studied by DLS and NMR. Microgel particles with different cross-linking densities were used to modify the network pore size and the response to temperature changes. The transition temperature was found to be basically independent of cross-linker density, (at low values), although the swelling ratio is very sensitive. The slight increase in the transition temperature for microgel particles having higher cross-linker concentrations is explained by the growing presence of the higher-solubility BA segments in the network. Only in the region of the transition temperature do water molecules feel confined, with their mobility decreasing as the mesh size decreases. Despite the fact that the fraction of bound water diminishes, the low relaxation time associated with those provokes the average relaxation time T_2 decreases. These changes in molecular diffusion in the transition region, are a direct consequence of changes in the molecular confinement. Hence these changes may be

regarded as a *molecular signature* of the volume phase transition. It would seem that the molecular diffusion is controlled only by the network size, and is independent of the actual mechanism controlling the network swelling (elasticity below the transition temperature or hydrophobicity above it). Molecule diffusion at low polymer compaction seems to be controlled by random thermal motion of solvent and the polymer chains (the "free volume" mechanism). However, for higher network densities, mesh obstructions control molecule mobility. The transition temperature, T_c, as defined in terms of the $D(T)$ inflection point, establishes the change of the diffusion mechanism.

Acknowledgment. This work was supported by the Spanish Government under Project MAT2003-03051-C03-01. B.S.M. thanks the Ministerio de Ciencia y Tecnología for a grant to enable an extended stay at the University of Bristol, where the NMR experiments were carried out. EPSRC is acknowledged for funding the NMR equipment.

References and Notes

(1) Heuberger, M.; Zäch, M.; Spencer, N. D. *Science* **2001**, *292*, 905.
(2) Mashl, R. J.; Joseph, S.; Aluru, N. R.; Jakobsson, E. *Nano Lett.* **2003**, *3*, 589.
(3) Huang, P.; Zhu, L.; Guo, Y.; Ge, Q.; Jing, A. J.; Chen, W. I.; Quirk, R. P.; Cheng, S. Z. D.; Thomas, E. L.; Lotz, B.; Hsiao, B. S.; Avila-Orta, C. A.; Sics, I. *Macromolecules* **2004**, *37*, 3689.
(4) Liu, Y.; Bishop, J.; Williams, L.; Blair, S.; Herron, J. *Nanotechnology* **2004**, *15*, 1368.
(5) Zhou, H.; Dill, K. A. *Biochemistry* **2001**, *40*, 11289.
(6) Anastasiadis, S. H.; Karatasos, K.; Vlachos, G. *Phys. Rev. Lett.* **2000**, *84*, 915.
(7) Lopez Cabarcos, E.; Rubio Retama, B. J.; Lopez Ruiz, B.; Heinrich, M.; Fernandez Barbero, A. *Physica A* **2004**, *344*, 417.
(8) Murthy, N.; Thng, Y. X.; Schuck, S.; Xu, M. C.; Frechet, J. M. *J. Am. Chem. Soc.* **2002**, *124*, 12398.
(9) Sanxia, L.; Anseth, K. S. *Macromolecules* **2000**, *33*, 2509.
(10) Dijk-Wolthius, W. N. E.; Hoogeboom, J. A. M.; Steenbergen, M. J.; Tsang, S. K. Y.; Hennink, W. E. *Macromolecules* **1997**, *30*, 4639.
(11) Griffiths, P. C.; Stilbs, P.; Chowdhry, B. Z.; Snowden, M. J. *Colloid Polym. Sci.* **1995**, *273*, 405.
(12) Guillermo, A.; Cohen Addad, J. P.; Bazile, J. P.; Duracher, D.; Elaissari, A.; Pichot, C. *J. Polym. Sci.* **2000**, *38*, 889.
(13) Kratz, K.; Hellweg, T.; Eimer, W. *Polymer* **2001**, *42*, 6631.
(14) Flory, P. J. *Principles of Polymer Chemistry*; Cornell University Press: London, 1953.
(15) Lele, A. K.; Hirve, M. M.; Badiger, M. V.; Mashelkar, R. A. *Macromolecules* **1997**, *30*, 157.
(16) Pelton, R. H.; Chibante, P. *Colloids Surf.* **1986**, *20*, 247.
(17) Crowther, H. M.; Vincent. B. *Colloid Polym. Sci.* **1998**, *276*, 46.
(18) Carr, H. Y.; Purcell, E. M. *Phy. Rev.* **1954**, *94*, 630.
(19) Meiboom, S.; Gill, D. *Rev. Sci. Instrum.* **1958**, *29*, 688.
(20) Van der Beek, G. P.; Cohen Stuart, M. A. *Langmuir* **1991**, *7*, 327.
(21) Mears, S. J.; Cosgrove, T.; Thompson, L.; Howell, I. *Langmuir* **1998**, *14*, 997.
(22) Zimmerman, J. R.; Brittin, W. E. *J. Phys. Chem.* **1957**, *61*, 1328.
(23) Smith, D. W.; Powles, J. G. *Mol. Phys.* **1966**, *10*, 451.
(24) Abragam, A. *The principles of nuclear magnetism*; Oxford University Press: Oxford, U.K., 1967.
(25) McClung, R. E. D.; Kivelson, D. *J. Chem. Phys.* **1968**, *49*, 3380.
(26) Hubbard, P. S. *Phys. Rev.* **1963**, *131*, 275.
(27) Price, W. S.; Kuchel, P. W.; Cornell, B. A. *Biophys. Chem.* **1989**, *33*, 205.
(28) Vold, R. R.; Sparks, S. W.; Vold, R. L. *J. Magn. Reson.* **1978**, *30*, 497.
(29) Jonas, J.; DeFries; Wilbur, D. J. *J. Chem. Phys.* **1976**, *65*, 582.
(30) Mills, R. *J. Phys. Chem.* **1973**, *77*, 685.
(31) Varga, I.; Gilányi, T.; Mészáros, R.; Filipcsei, G.; Zrínyi, M. *J. Phys. Chem. B* **2001**, *105*, 9071.
(32) Hellweg, T.; Dewhurst, C. D.; Brückner, E.; Kratz, K.; Eimer, W. *Colloid Polym. Sci.* **2000**, *278*, 972.
(33) Senff, H.; Richtering, W. *Colloid Polym. Sci.* **2000**, *278*, 830.
(34) Dong, L. C.; Hoffman, A. S. *Proc. Int. Symp. Control. Release Bioact. Matter* **1990**, *17*, 325.
(35) Yasuda, H.; Lamaze, C. E.; Ikenberry, L. D. *Makromol. Chem.* **1968**, *118*, 19.
(36) Ogston, A. G.; Preston, B. N.; Well, J. D. *Proc. R. Soc.* **1973**, *A333*, 297.
(37) Fernández-Barbero, A.; Fernández-Nieves, A.; Grillo, I.; López-Cabarcos, E. *Phys. Rev. E* **2002**, *66*, 51803.

MA0510284